Inorganic Chemistry

pubs.acs.org/IC

Communication

Racemization Pathway for $MoO_2(acac)_2$ Favored over Ray−Dutt, Bailar, and Conte−Hippler Twists

George Dhimba, Alfred Muller, and Koop Lammertsma*

Cite This: *Inorg. Chem.* 2022, 61, 14918−14923

Read Online

ACCESS | Metrics & More | Article Recommendations | Supporting Information

ABSTRACT: Chiral *cis*-$MoO_2(acac)_2$ racemizes via four pathways that agree with and extend upon Muetterties' topological analysis for dynamic $MX_2(chel)_2$ complexes. Textbook Ray−Dutt and Bailar twists are the least favored with barriers of 27.5 and 28.7 kcal/mol, respectively. Rotating both acac ligands of the Bailar structure by 90° gives the lower Conte−Hippler twist (20.0 kcal/mol), which represents a valley−ridge inflection that invokes the trans isomer. The most favorable is a new twist that was found by 90° rotation of only one acac ligand of the Bailar structure. The gas-phase barrier of 17.4 kcal/mol for this Dhimba−Muller−Lammertsma twist further decreases upon inclusion of the effects of solvents to 16.3 kcal/mol (benzene), 16.2 kcal/mol (toluene), and 15.4 kcal/mol (chloroform), which are in excellent agreement with the reported experimental values.

Rationally designed catalysts capable of effecting enantioselective chemical transformations are crucial to satisfying the growing industrial demand for chiral fine chemicals.[1] Despite the tremendous advances in asymmetric organocatalysis, as highlighted by the 2021 Nobel Prize in Chemistry,[2] most catalysts used for the conversions of organic compounds are still transition-metal complexes with ligands coming from the ever-growing chiral pool.[3] These chiral ligands are considered to be responsible for the transfer of chirality to the reaction product, but the elaborate syntheses and unpredictable enantioselectivity are limiting factors. An alternative is to solely use the stereogenicity of the metal center by the enantiomeric chelation of achiral ligands around the coordinating transition metal.[4]

Octahedral chiral complexes are, in fact, known as far back as 1911 when Werner reported on $[Co(en)_3]^{3+}$ (en = ethylenediamine);[5] $[Cr(en)_3]^{3+}$, $[Rh(en)_3]^{3+}$, $[Ir(en)_3]^{3+}$, and $[Pt(en)_4]^{4+}$ were described shortly thereafter.[6] Werner's D_{3d}-symmetrical cobalt(III) complexes carrying three simple achiral bidentate ligands were revived recently by Gladysz et al., demonstrating their effectiveness as enantioselective catalysts.[7] In 2003, Fontecave et al. introduced the term "chiral-at-metal" catalysis and showed modest enantioselectivity for the asymmetric transfer hydrogenation and asymmetric oxidation of sulfides using $[Ru(dmp)_2(CH_3CN)_2]^{2+}$ (dmp = 2,9-dimethyl-1,10-phenanthroline).[8] The field of chiral-at-metal catalysis was expanded majorly in the past decade by Meggers et al., who reported many different asymmetric catalytic reactions with high enantioselectivity using chiral rhodium(III) and iridium(III), $[M(tbpb)_2(CH_3CN)_2]^+$ (M = Rh, Ir; tbpb = 5-*tert*-butyl-2-phenylbenzoxazole),[9] and recently with similar chiral iron(II) complexes.[10]

The asymmetric Lewis acid transition-metal complexes, carrying two bidentate and two acetonitrile ligands, apparently have high energy barriers of racemization, which enable the catalysts to maintain their chiral integrity. However, retention of chirality for other transition-metal complexes is a priori not evident because of the configurational flexibility at the metal center.[11] Whereas such dynamics can be restricted by bi-, tri-, and tetradentate ligands, racemization is of general concern in chiral-at-metal systems. The crux is to recognize and control the dynamic pathways.

Already half a century ago, in-depth topological studies by Muetterties revealed the complexity by which penta- and hexacoordinate systems racemize.[12] He also showed that the number of racemization pathways reduces with bidentate ligands. Illustrative is the reduction of 20 feasible permutations of a pentacoordinate system, which can be described in a Levi−Desargues graph, by introducing two bulky bidentate ligands.[13] These cause the energy barriers for Berry pseudorotation to increase and prohibit racemization, as is the case for silicate $[Si(pn)_2F]^-$ [pn = 2-(phenyl)naphthyl].[14] Octahedral complexes are subject to a far larger number of permutations, which also reduce upon chelation. Well-established racemization pathways for trischelate complexes are the Ray−Dutt[15] and Bailar[16] twists in which the chelating ligands undergo a C_3 rotation[17] via rhombic (D_{3h} symmetry) and trigonal-prismatic (C_{2v} symmetry) transition states, respectively (Figure 1).[18] Rarer pathways include the dancing-Bailar twist,[19] those with a bicapped tetrahedral structure,[20] and those invoking pentacoordination.[21] Besides Muetterties' topological studies, little is known about the racemization pathways of octahedral complexes with two bidentate ligands, which is the subject of the present study that focuses on *cis*-$MoO_2(acac)_2$ (acac = acetylacetonate).

Received: March 12, 2022
Published: August 18, 2022

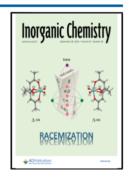

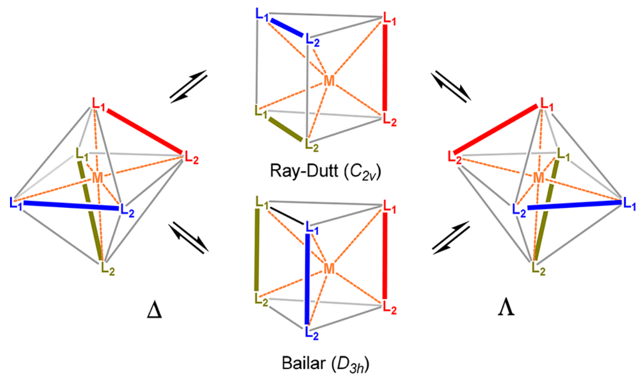

Figure 1. Ray−Dutt and Bailar twists by which chiral octahedral complexes undergo racemization. The three bidentate ligands are shown in blue, green, and red. The gray lines complement the edges of the octahedral and trigonal-prismatic structures, with the orange dashed lines representing the transition-metal coordination sites.

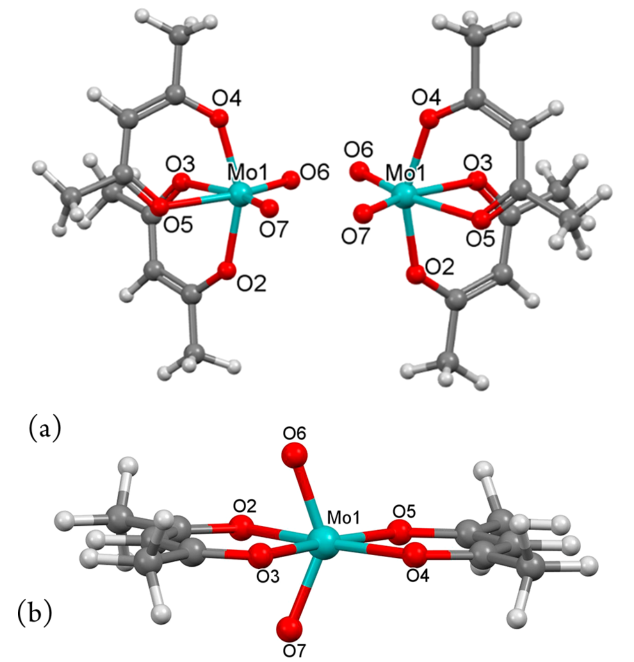

Figure 2. (a) Δ and Λ enantiomers of *cis*-$MoO_2(acac)_2$ and (b) *trans*-$MoO_2(acac)_2$.

cis-$MoO_2(acac)_2$ is an effective catalyst for epoxidizing olefins with peroxides, but we are not aware of asymmetric homogeneous catalysis with one of its enantiomers.[22] The solid-state structure has been reported for the racemic mixture[23] and for an enantiomer of a derivative.[22b] Conte and Hippler determined by variable ^{1}H NMR spectroscopy a modest activation energy E_a of 16.9 kcal/mol for the racemization of *cis*-$MoO_2(acac)_2$ in benzene, 13.7 kcal/mol in chloroform, and 15.1 kcal/mol in toluene, indicating a small solvation effect.[24] These barriers are similar to those reported by the group of Wise in 1971.[25] SOGGA11-X/LANL2DZ +G** calculations by Conte and Hippler gave E_0 barriers of 26.7 and 27.2 kcal/mol for the Ray−Dutt and Bailar twists and a lower, but still sizable, barrier of 19.4 kcal/mol for a different pathway; the heights of the barriers were not affected by inclusion of the effect of solvents. The magnitudes of these barriers seem to indicate that the racemization of *cis*-$MoO_2(acac)_2$ cannot be attributed to the Bailar or Ray−Dutt twists and likely not to the twist suggested by Conte and Hippler. Therefore, in the context of the topological analysis of $MX_2(chel)_2$ systems, we felt that a theoretical study on the racemization pathways is in order.

The potential energy surface for the $MoO_2(acac)_2$ complex was examined with *Gaussian 16*, version B01,[26] using the hybrid meta-generalized-gradient-approximation functional ωB97X-D,[27] which incorporates empirical dispersion terms and long-range interactions,[28] and the 6-31G(d) basis set for C, H, and O and *LANL2DZ* for Mo.[29] The reported absolute electronic energies for all optimized structures were estimated by single-point calculation with the 6-311+G(2d,p) basis set. Frequency and intrinsic-reaction-coordinate (IRC) calculations confirmed the nature of each transition structure.[30] The effect of solvation was estimated by single-point calculations with the polarizable continuum solvent model at 25 °C.[31]

The geometries of Λ- and Δ-*cis*-$MoO_2(acac)_2$, shown in Figure 2, have a distorted octahedral arrangement in which the planes formed by the acac ligands and metal center are each tilted by 10.8° from orthogonality with the MoO_2 plane. The Mo═O bonds of the MoO_2 fragment have a length of 1.692 Å and an angle of 104.6°. The two Mo−O bonds of each acac ligand are longer and unequal to each other, i.e., 2.019 Å ($Mo-O_{cis}$) and 2.252 Å ($Mo-O_{trans}$), because of the different chemical environments of the two acac oxygen atoms. The methyl groups of the acac ligands are eclipsed with the methine hydrogen atoms. The geometry of Λ/Δ-*cis*-$MoO_2(acac)_2$ compares well with those of the reported X-ray crystal structures.[23]

trans-$MoO_2(acac)_2$ (C_{2v} symmetry), shown in Figure 2b, is a substantial 50.6 kcal/mol less stable than the cis isomer. It is then not surprising that no solid-state structure is known for this isomer. Moreover, geometry optimization with the extended basis set suggests it to be a transition structure (C_{2v} symmetry) at a flat energy plateau with an imaginary frequency of a mere −12 cm^{-1}. The trans Mo═O bonds of its MoO_2 fragment are longer (1.731 Å) than those in the cis isomer and deviate substantially from linearity (140.0°), and both tilt toward one of the acac ligands, which has as a result longer Mo−O bonds (2.137 Å) than the other ligand (2.034 Å).

To understand the racemization of *cis*-$MoO_2(acac)_2$ and the potential role of the trans isomer, it is instructive to analyze their topological relationship. Muetterties showed that a metal complex with six different (monodentate) ligands has 30 octahedral isomers and 120 trigonal-prismatic iosomers but that this reduces significantly for complexes with two symmetrical bidentate ligands, $MX_2(chel)_2$. Figure 3, adapted from the original study, gives the topological representation, showing the enantiomeric cis isomers at the base and the trans isomer at the apex of an isosceles triangle (open dots). The closed dots at the edges of the triangle are the trigonal-prismatic structures (Figure 3, right), embodying rearrangement of the octahedral structures.

Topological analysis gives three direct racemization pathways for *cis*-$MX_2(chel)_2$, each with a trigonal-prismatic transition structure (cis_a, cis_b, and trans in Figure 3), complemented by a pathway via the trans isomer that involves a set of enantiomeric structures (d,l trans). We are unaware whether all of these racemization pathways have found solid footing in the literature. Consequently, we felt $MoO_2(acac)_2$ was ideal to verify topological analysis in the context of

https://doi.org/10.1021/acs.inorgchem.2c00824
Inorg. Chem. 2022, 61, 14918−14923

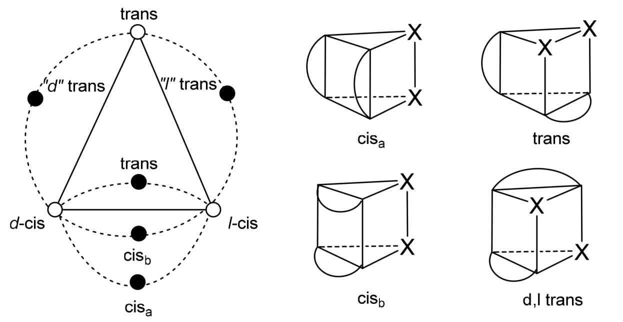

Figure 3. Topological representation of $MX_2(chel)_2$ with octahedral structures (open dots) and connecting trigonal-prismatic structures (closed dots) shown separately.

comparing the racemization barriers of the cis isomer with the reported experimental one.

The obvious places to start with are the established Ray–Dutt and Bailar twists for trischelating octahedral systems (Figure 1), which are represented respectively as cis$_b$ and cis$_a$ in Figure 3. Their corresponding C_{2v}-symmetric transition structures for $MoO_2(acac)_2$ (Figure 4) have relative energies of

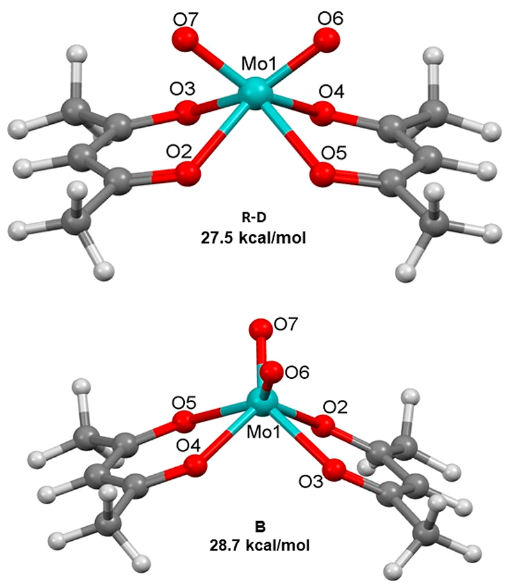

Figure 4. Ray–Dutt (top) and Bailar (bottom) transition structures for the racemization of *cis*-$MoO_2(acac)_2$.

a significant 27.5 and 28.7 kcal/mol, respectively. The structure for the Ray–Dutt twist has its MoO_2 unit ($d_{Mo=O}$ = 1.696 Å; $\angle_{OMoO}$ = 97.4°) bisecting both virtually planar acac ligands (d_{Mo-O} = 2.128 Å), which have an intercept angle of 19.6°. In the Bailar transition structure, the MoO_2 unit ($d_{Mo=O}$ = 1.687 Å; $\angle_{OMoO}$ = 95.8°) is rotated by 90° and has a larger bisecting angle of 48.3° between the acac ligands (d_{Mo-O} = 2.148 Å).

Next, we focus on the role of *trans*-$MoO_2(acac)_2$ in isomerization of the cis isomer and on how the d,l trans forms (Figure 3) are involved. The latter can be considered to result from the Bailar transition structure by 90° rotation of both acac ligands. Such a transformation gives indeed a transition structure (Figure 5) with a relative energy of 20.0 kcal/mol, akin to that reported by Conte and Hippler.[31] The two planar acac ligands of the C_{2v}-symmetric structure lie in the same plane, with each having Mo–O bonds of 2.040 and

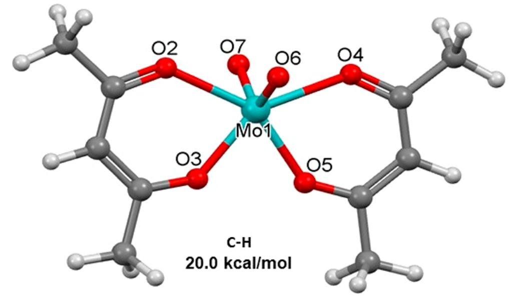

Figure 5. Conte–Hippler transition structure for the racemization of *cis*-$MoO_2(acac)_2$.

2.264 Å to the MoO_2 unit ($d_{Mo=O}$ = 1.693 Å; $\angle_{OMoO}$ = 117.2°). The IRC confirms that this transition structure is yet another structure for the racemization of *cis*-$MoO_2(acac)_2$ (see the Supporting Information) by opposite rotation of the acac ligands, but it still does not match the reported experimental value.

Further inspection of the C_{2v}-symmetric structure is revealing. Rotating the MoO_2 plane that bisects the two acac ligands by 90° and enlarging the O=Mo=O angle (117.2° → 140.0°) results in C_{2v}-symmetric *trans*-$MoO_2(acac)_2$ (Figure 2b). This rotation can be left- or right-handed so that the MoO_2 unit gets directed toward either one or the other acac ligand, which is in accordance with topological analysis (Figure 3). The high-energy trans isomer lies on a very flat high-energy plateau that allows for slight bending of its acac ligands. Despite the technical difficulties that this caused, we obtained an IRC that connects *trans*-$MoO_2(acac)_2$ by left- and right-handed rotation of the MoO_2 unit to the Conte–Hippler transition structure (Figure 5) and thus ultimately to Δ- and Λ-*cis*-$MoO_2(acac)_2$. Evidently, this transition structure is a valley–ridge inflection point that gives one *cis*-$MoO_2(acac)_2$ enantiomer when the IRC is followed in one direction, likely because of torque selectivity.[32] The relationship is shown in a simplified manner in Figure 6.

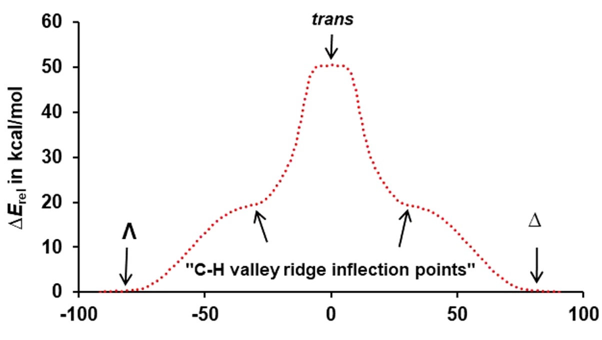

Figure 6. IRC for *trans*-$MoO_2(acac)_2$.

The only remaining racemization pathway to consider is that of the trans form in Figure 3. This twist is readily conceived by rotating one of the chelates of cis$_a$ by 90° instead of both. Such a rotation of one acac ligand of the Bailar structure led, in fact, to the hitherto unknown transition structure shown in Figure 7. Tracing the IRC trajectory confirms that it represents a new racemization pathway for *cis*-$MoO_2(acac)_2$ (see Figure S1). The two planar acac ligands of the structure lie in the orthogonal planes, with one having two symmetrical $d_{Mo=O}$ bonds (2.176 Å) and the other two unsymmetrical bonds (2.108 and 2.120 Å) to the MoO_2 unit ($d_{Mo=O}$ = 1.687 Å;

https://doi.org/10.1021/acs.inorgchem.2c00824
Inorg. Chem. 2022, 61, 14918–14923

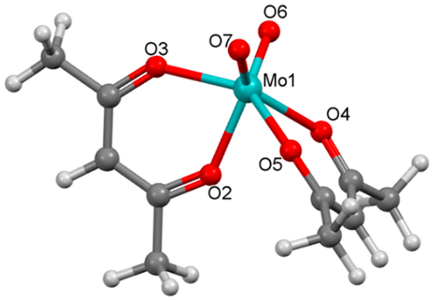

Figure 7. D−M−L transition structure for the racemization of *cis*-$MoO_2(acac)_2$.

$\angle_{OMoO}$ = 101.1°). Most importantly, this new transition structure reflects the lowest-energy barrier for the racemization of *cis*-$MoO_2(acac)_2$ with a barrier of only 17.4 kcal/mol and on including the effects of solvation of 16.3 kcal/mol (benzene), 16.2 kcal/mol (toluene), and 15.4 kcal/mol (chloroform). The calculated barriers for these different solvent systems compare exceptionally well with the experimental E_a values of 16.9 kcal/mol (benzene), 15.1 kcal/mol (toluene), and 13.7 kcal/mol (chloroform), which were determined by Conte and Hippler.[24] Evidently, this new twist represents the most favorable pathway by which the enantiomers of *cis*-$MoO_2(acac)_2$ racemize.

In conclusion, the four pathways by which Δ- and Λ-*cis*-$MoO_2(acac)_2$ can racemize are the Ray−Dutt and Bailar twists and those in which one or both chelates of the Bailar twist are rotated by 90° (Figure 8). The barrier of 17.4 kcal/mol for the

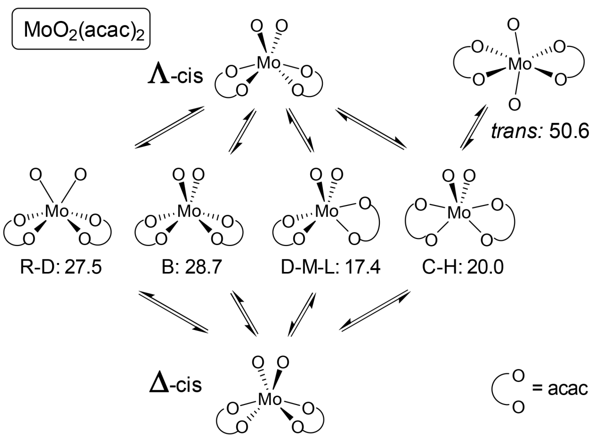

Figure 8. Schematic presentation of the racemization pathways for (nonsolvated) *cis*-$MoO_2(acac)_2$ with relative energies (kcal/mol) for the Ray−Dutt (R−D), Bailar (B), Dhimba−Muller−Lammertsma (D−M−L), and Conte−Hippler (C−H) transition structures and the trans isomer.

pathway with one rotated acac ligand, the Dhimba−Muller−Lammertsma (D−M−L) twist, agrees excellently with that determined experimentally. The less favored C−H twist in which both acac ligands are rotated represents a valley−ridge inflection that invokes the trans isomer. The well-established Ray−Dutt and Bailar twists are by far the least favored pathways. The obtained results agree fully with Muetterties' topological analysis and give confidence that they apply to all dynamic $MX_2(chel)_2$ complexes. Inhibiting racemization of such complexes with properly substituted bidentate ligands can propel asymmetric catalysis with chiral-at-metal catalysts derived from readily available, inexpensive transition metals, which we are currently exploring.

■ ASSOCIATED CONTENT

Supporting Information

The Supporting Information is available free of charge at https://pubs.acs.org/doi/10.1021/acs.inorgchem.2c00824.

All computational details (PDF)

■ AUTHOR INFORMATION

Corresponding Author

Koop Lammertsma − *Department of Chemical Sciences, University of Johannesburg, Auckland Park, Johannesburg 2006, South Africa; Department of Chemistry and Pharmaceutical Sciences, Faculty of Sciences, Vrije Universiteit Amsterdam, Amsterdam 1081 HZ, The Netherlands;* orcid.org/0000-0001-9162-5783; Email: K.Lammertsma@vu.nl

Authors

George Dhimba − *Department of Chemical Sciences, University of Johannesburg, Auckland Park, Johannesburg 2006, South Africa*

Alfred Muller − *Department of Chemical Sciences, University of Johannesburg, Auckland Park, Johannesburg 2006, South Africa;* orcid.org/0000-0003-2304-6987

Complete contact information is available at: https://pubs.acs.org/10.1021/acs.inorgchem.2c00824

Author Contributions

All authors discussed the results and contributed to the final manuscript.

Notes

The authors declare no competing financial interest.

■ ACKNOWLEDGMENTS

We gratefully acknowledge support of the National Research Foundation (Grant 120842) and the Centre for High Performance Computing of South Africa. We thank Dr. J. E. Borger for the initial calculations.

■ REFERENCES

(1) Walsh, P. J.; Kozlowski, M. C. *Fundamentals of Asymmetric Catalysis*; University Science Books: Sausalito, CA, 2009.

(2) The Nobel Prize in Chemistry 2021 was awarded jointly to B. List and D. W. C. MacMillan "for the development of asymmetric organocatalysis". www.nobelprize.org/prizes/chemistry/2021/summary.

(3) Illustrative for chiral phosphorus-based ligands are: (a) *Phosphorus(III) Ligands inHomogeneous Catalysis:Design and Synthesis*; van Leeuwen, P. W. N. M., Kamer, P. C. J., Eds.; Wiley, 2012. (b) *Phosphorus Ligands in Asymmetric Catalysis*; Börner, A., Ed.; Wiley-VCH: Weinheim, Germany, 2008. (c) Guo, H.; Fan, Y. C.; Sun, Z.; Wu, Y.; Kwon, O. Phosphine Organocatalysis. *Chem. Rev.* **2018**, *118*, 10049−10293. (d) Grabulosa, A. *P-Stereogenic Ligands in Enantioselective Catalysis*; RSC Publishing: Cambridge, U.K., 2011. (e) Cabré, A.; Riera, A.; Verdaguer, X. P-Stereogenic Amino-Phosphines as Chiral Ligands: From Privileged Intermediates to Asymmetric Catalysis. *Acc. Chem. Res.* **2020**, *53*, 676−689.

(4) (a) Bauer, E. B. Chiral-at-metal complexes and their catalytic applications in organic synthesis. *Chem. Soc. Rev.* **2012**, *41*, 3153−3167. (b) Malcolmson, S. J.; Meek, S. J.; Sattely, E. S.; Schrock, R. R.; Hoveyda, A. H. Highly efficient molybdenum-based catalysts for enantioselective alkene metathesis. *Nature* **2008**, *456*, 933−937.

(c) Gong, L.; Chen, L.-A.; Meggers, E. Asymmetric Catalysis Mediated by the Ligand Sphere of Octahedral Chiral-at-Metal Complexes. *Angew. Chem., Int. Ed.* **2014**, *53*, 10868−10874. (d) Fontecave, M.; Hamelin, O.; Menage, S. Chiral-at-metal complexes as asymmetric catalysts. In Chiral Diazaligands for Asymmetric Synthesis. *Top. Organomet. Chem.* **2005**, *15*, 271−288. (e) Knight, P. D.; Scott, P. Predetermination of chirality at octahedral centres with tetradentate ligands: prospects for enantioselective catalysis. *Coord. Chem. Rev.* **2003**, *242*, 125−143. (f) Fusi, G. M.; Gazzola, S.; Piarulli, U. Chiral Iron Complexes in Asymmetric Organic Transformations. *Adv. Synth. Catal.* **2022**, *364*, 696−714. (g) Tandura, S. N.; Shumsky, A. N.; Ugrak, B. I.; Negrebetsky, V. V.; Bylikin, S. Y.; Kolesnikov, S. P. Stereochemical flexibility of bis (amidomethyl) dichlorogermanes. A novel dissociative mechanism of ligand exchange in neutral hexacoordinated bischelate complexes. *Organometallics* **2005**, *24*, 5227−5240.

(5) Werner, A. Zur Kenntnis des asymmetrischen Kobaltatoms. I. Ber. *Dtsch. Chem. Ges.* **1911**, *44*, 1887−1898. (b) Werner, A. Zur Kenntnis des asymmetrischen Kobaltatoms. II. *Ber. Dtsch. Chem. Ges.* **1911**, *44*, 2445−2455. (c) Werner, A. Zur Kenntnis des asymmetrischen Kobaltatoms. III. *Ber. Dtsch. Chem. Ges.* **1911**, *44*, 3272−3278. (d) Werner, A. Zur Kenntnis des asymmetrischen Kobaltatoms. IV. *Ber. Dtsch. Chem. Ges.* **1911**, *44*, 3279−3284. (e) Werner, A. Zur Kenntnis des asymmetrischen Kobaltatoms. V. *Ber. Dtsch. Chem. Ges.* **1912**, *45*, 121−130.

(6) (a) Werner, A. Über Spiegelbildisomerie bei Chromverbindungen. *Ber. Dtsch. Chem. Ges.* **1912**, *45*, 865−869. (b) Werner, A. Über Spiegelbildisomerie bei Rhodium-Verbindungen. *I. Ber. Dtsch. Chem. Ges.* **1912**, *45*, 1228−1236. (c) Werner, A.; Smirnoff, A. P. Über optischaktive Iridiumverbindungen. *Helv. Chim. Acta* **1920**, *3*, 472−486. (d) Werner, A. Über Spiegelbildisomerie bei Platinverbindungen I. Vierteljahresschr. *Naturforsch. Ges. Zürich* **1917**, *62*, 553−564.

(7) Wegener, A. R.; Kabes, C. Q.; Gladysz, J. A. Launching Werner Complexes into the Modern Era of Catalytic Enantioselective Organic Synthesis. *Acc. Chem. Res.* **2020**, *53*, 2299−2313.

(8) (a) Chavarot, M.; Ménage, S.; Hamelin, O.; Charnay, F.; Pécaut, J.; Fontecave, M. Chiral-at-Metal" Octahedral Ruthenium(II) Complexes with Achiral Ligands: A New Type of Enantioselective Catalyst. *Inorg. Chem.* **2003**, *42*, 4810−4816. (b) Hamelin, O.; Rimboud, M.; Pécaut, J.; Fontecave, M. Chiral-at-Metal Ruthenium Complex as a Metalloligand for Asymmetric Catalysis. *Inorg. Chem.* **2007**, *46*, 5354−5360.

(9) (a) Huang, X.; Meggers, E. Asymmetric Photocatalysis with Bis-cyclometalated Rhodium Complexes. *Acc. Chem. Res.* **2019**, *52*, 833−847. (b) Zhang, L.; Meggers, E. Steering Asymmetric Lewis Acid Catalysis Exclusively with Octahedral Metal-Centered Chirality. *Acc. Chem. Res.* **2017**, *50*, 320−330.

(10) (a) Hong, Y.; Jarrige, L.; Harms, K.; Meggers, E. Chiral-at-Iron Catalyst: Expanding the Chemical Space for Asymmetric Earth-Abundant Metal Catalysis. *J. Am. Chem. Soc.* **2019**, *141*, 4569−4572. (b) Hong, Y.; Cui, T.; Ivlev, S.; Xie, X.; Meggers, M. Chiral-at-Iron Catalyst for Highly Enantioselective and Diastereoselective Hetero-Diels-Alder Reaction. *Chem. Eur. J.* **2021**, *27*, 8557−8563.

(11) (a) Alvarez, S. Distortion Pathways of Transition Metal Coordination Polyhedra Induced by Chelating Topology. *Chem. Rev.* **2015**, *115*, 13447−13483. (b) Dowley, P.; Garbett, K.; Gillard, R. D. Isorotatory points and racemization. *Inorg. Chim. Acta* **1967**, *1*, 278−280. (c) Lawrance, G. A.; Stranks, D. R. Volumes of activation for intramolecular racemization mechanisms. High-pressure racemization of bipyridyl, phenanthroline and oxalato complexes of chromium(III) in solution. *Inorg. Chem.* **1977**, *16*, 929−935. (d) Riblet, F.; Novitchi, G.; Scopelliti, R.; Helm, L.; Gulea, A.; Merbach, A. E. Isomerization Mechanisms of Stereolabile tris- and bis-Bidentate Octahedral Cobalt(II) Complexes: X-ray Structure and Variable Temperature and Pressure NMR Kinetic Investigations. *Inorg. Chem.* **2010**, *49*, 4194−4211.

(12) (a) Muetterties, E. L. Intramolecular rearrangement of six-coordinate structures. *J. Am. Chem. Soc.* **1968**, *90*, 5097−5102. (b) Muetterties, E. L. Topological representation of stereoisomerism. I. Polytopal rearrangements. *J. Am. Chem. Soc.* **1969**, *91*, 1636−1643. (c) Muetterties, E. L. Topological representation of stereoisomerism. II. The five-atom family. *J. Am. Chem. Soc.* **1969**, *91*, 4115−4142.

(13) Couzijn, E. P. A.; Slootweg, J. C.; Ehlers, A. W.; Lammertsma, K. Stereomutation of pentavalent compounds. validating the Berry pseudorotation, redressing the Ugi's turnstile rotation, and revealing the two- and three-gated turnstiles. *J. Am. Chem. Soc.* **2010**, *132*, 18127−18140.

(14) Van Der Boon, L. J.; Van Gelderen, L.; De Groot, T. R.; Lutz, M.; Slootweg, J. C.; Ehlers, A. W.; Lammertsma, K. Chiral control in pentacoordinate systems: The case of organosilicates. *Inorg. Chem.* **2018**, *57*, 12697−12708.

(15) Ray, P.; Dutt, N. Kinetics and mechanism of racemization of optically active cobaltic trisbiguanide complex. *J. Indian Chem. Soc.* **1943**, *20*, 81−92.

(16) Bailar, J. C. Some problems in the stereochemistry of coordination compounds: Introductory lecture. *J. Inorg. Nucl. Chem.* **1958**, *8*, 165−175.

(17) (a) Casanova, D.; Cirera, J.; Llunell, M.; Alemany, P.; Avnir, D.; Alvarez, S. Minimal Distortion Pathways in Polyhedral Rearrangements. *J. Am. Chem. Soc.* **2004**, *126*, 1755−1763. (b) Amati, M.; Lelj, F. Competition between Bailar and Ray-Dutt paths in conformational interconversion of tris-chelated complexes: a DFT study. *Theor. Chem. Acc.* **2008**, *120*, 447−457.

(18) (a) Davis, A. V.; Firman, T. K.; Hay, B. P.; Raymond, K. N. d-Orbital Effects on Stereochemical Non-Rigidity: Twisted TiIV Intramolecular Dynamics. *J. Am. Chem. Soc.* **2006**, *128*, 9484−9496. (b) Rikkou, M.; Manos, M.; Tolis, E.; Sigalas, M. P.; Kabanos, T. A.; Keramidas, A. D. NMR and theoretical investigations on the structures and dynamics of octahedral bis (chelate) dichloro VIII compounds isolated by an unusual reduction of non-oxo VIV species. *Inorg. Chem.* **2003**, *42*, 4640−4649.

(19) Ashley, D. C.; Jakubikova, E. Ray-Dutt and Bailar Twists in Fe (II)-Tris (2, 2′-bipyridine): Spin States, Sterics, and Fe−N Bond Strengths. *Inorg. Chem.* **2018**, *57*, 5585−5596.

(20) Hoffmann, R.; Howell, J. M.; Rossi, A. R. Bicapped tetrahedral, trigonal prismatic, and octahedral alternatives in main and transition group six-coordination. *J. Am. Chem. Soc.* **1976**, *98*, 2484−2492.

(21) Foreman, M. R. S. J.; Hill, A. F.; White, A. J. P.; Williams, D. J. Hydrotris(methimazolyl)borato Alkylidyne Complexes of Tungsten. *Organometallics* **2003**, *22*, 3831−3840.

(22) (a) Annese, C.; Caputo, D.; D'Accolti, L.; Fusco, C.; Nacci, A.; Rossin, A.; Tuci, G.; Giambastiani, G. Dioxomolybdenum (VI) Complexes with Salicylamide Ligands: Synthesis, Structure, and Catalysis in the Epoxidation of Olefins under Eco-Friendly Conditions. *Eur. J. Inorg. Chem.* **2019**, *2019*, 221−229. (b) Korstanje, T. J.; Folkertsma, E.; Lutz, M.; Jastrzebski, J. T.; Klein Gebbink, R. J. Synthesis, Characterization, and Catalytic Behavior of Dioxomolybdenum Complexes Bearing AcAc-Type Ligands. *Eur. J. Inorg. Chem.* **2013**, *2013*, 2195−2204. (c) Shen, Y.; Jiang, P.; Wai, P. T.; Gu, Q.; Zhang, W. Recent progress in application of molybdenum-based catalysts for epoxidation of alkenes. *Catalysts* **2019**, *9*, 31. (d) Kühn, F. E.; Santos, A. M.; Abrantes, M. Mononuclear Organomolybdenum-(VI) Dioxo Complexes: Synthesis, Reactivity, and Catalytic Applications. *Chem. Rev.* **2006**, *106*, 2455−2475. (e) Barlan, A. U.; Basak, A.; Yamamoto, H. Enantioselective Oxidation of Olefins Catalyzed by a Chiral Bishydroxamic Acid Complex of Molybdenum. *Angew. Chem., Int. Ed.* **2006**, *45*, 5849−5852.

(23) (a) Kamenar, B.; Penavic, M.; Prout, C. K. Dioxobis(2,4-pentanedionato)molybdenum(VI), $C_{10}H_{14}MoO_6$. *Cryst. Struct. Commun.* **1973**, *2*, 41−44. (b) Krasochka, O. N.; Sokolova, Yu. A.; Atovmyan, L. O. Crystal and Molecular Structures of Molybdenum bis-Acetylacetonate, $MoO_2(C_5H_7O_2)_2$, Zh. *Strukt. Khim. (Russ.) (J. Struct. Chem.)* **1975**, *16*, 696−698. (c) Johnston, D. H.; King, C.; Seitz, A.; Sethi, M. Bis(2,4-dioxopentan-3-ido-j2O,O000)dioxidomolybdenum(VI): a redetermination. *IUCrData* **2021**, *6*, x210778.

(24) Conte, M.; Hippler, M. Dynamic NMR and quantum-chemical study of the stereochemistry and stability of the chiral MoO2 (acac) 2 complex in solution. *J. Phys. Chem. A* **2016**, *120*, 6677−6687.

(25) Craven, B. M.; Ramey, K. C.; Wise, W. B. Lability and Stereochemistry of Dioxobis(2,4-pentanedionato)molybdenum (VI). *Inorg. Chem.* **1971**, *10*, 2626−2628.

(26) Frisch, M. J.; Trucks, G. W.; Schlegel, H. B.; Scuseria, G. E.; Robb, M. A.; Cheeseman, J. R.; Scalmani, G.; Barone, V.; Petersson, G. A.; Nakatsuji, H.; Li, X.; Caricato, M.; Marenich, A. V.; Bloino, J.; Janesko, B. G.; Gomperts, R.; Mennucci, B.; Hratchian, H. P.; Ortiz, J. V.; Izmaylov, A. F.; Sonnenberg, J. L.; Williams-Young, D.; Ding, F.; Lipparini, F.; Egidi, F.; Goings, J.; Peng, B.; Petrone, A.; Henderson, T.; Ranasinghe, D.; Zakrzewski, V. G.; Gao, J.; Rega, N.; Zheng, G.; Liang, W.; Hada, M.; Ehara, M.; Toyota, K.; Fukuda, R.; Hasegawa, J.; Ishida, M.; Nakajima, T.; Honda, Y.; Kitao, O.; Nakai, H.; Vreven, T.; Throssell, K.; Montgomery, J. A., Jr.; Peralta, J. E.; Ogliaro, F.; Bearpark, M. J.; Heyd, J. J.; Brothers, E. N.; Kudin, K. N.; Staroverov, V. N.; Keith, T. A.; Kobayashi, R.; Normand, J.; Raghavachari, K.; Rendell, A. P.; Burant, J. C.; Iyengar, S. S.; Tomasi, J.; Cossi, M.; Millam, J. M.; Klene, M.; Adamo, C.; Cammi, R.; Ochterski, J. W.; Martin, R. L.; Morokuma, K.; Farkas, O.; Foresman, J. B.; Fox, D. J. *Gaussian 09*, R. A.; *Gaussian 16*, revision C.01; Gaussian, Inc.: Wallingford, CT, 2009 and 2016, Vol. *121*, pp 150−166.

(27) Chai, J.-D.; Head-Gordon, M. Long-range corrected hybrid density functionals with damped atom−atom dispersion corrections. *Phys. Chem. Chem. Phys.* **2008**, *10*, 6615−6620.

(28) Minenkov, Y.; Singstad, Å.; Occhipinti, G.; Jensen, V. R. The accuracy of DFT-optimized geometries of functional transition metal compounds: a validation study of catalysts for olefin metathesis and other reactions in the homogeneous phase. *Dalton Trans.* **2012**, *41*, 5526−5541.

(29) (a) Couty, M.; Hall, M. B. Basis sets for transition metals: Optimized outer p functions. *J. Comput. Chem.* **1996**, *17*, 1359−1370. (b) Yang, Y.; Weaver, M. N.; Merz, K. M. Assessment of the "6-31+G** + LANL2DZ" Mixed Basis Set Coupled with Density Functional Theory Methods and the Effective Core Potential: Prediction of Heats of Formation and Ionization Potentials for First-Row-Transition-Metal Complexes. *J. Phys. Chem. A* **2009**, *113*, 9843−9851. (c) Hay, P. J.; Wadt, W. R. Ab initio effective core potentials for molecular calculations. Potentials for the transition metal atoms Sc to Hg. *J. Chem. Phys.* **1985**, *82*, 270−283.

(30) (a) Gonzalez, C.; Schlegel, H. B. An improved algorithm for reaction path following. *J. Chem. Phys.* **1989**, *90*, 2154−2161. (b) Gonzalez, C.; Schlegel, H. B. Reaction path following in mass-weighted internal coordinates. *J. Phys. Chem.* **1990**, *94*, 5523−5527.

(31) (a) Barone, V.; Cossi, M. Quantum Calculation of Molecular Energies and Energy Gradients in Solution by a Conductor Solvent Model. *J. Phys. Chem. A* **1998**, *102*, 1995−2001. (b) Barone, V.; Cossi, M.; Tomasi, J. Geometry optimization of molecular structures in solution by the polarizable continuum model. *J. Comput. Chem.* **1998**, *19*, 404−417. (c) Cossi, M.; Rega, N.; Scalmani, G.; Barone, V. Energies, structures, and electronic properties of molecules in solution with the C-PCM solvation model. *J. Comput. Chem.* **2003**, *24*, 669−681.

(32) Jefford, C. W.; Bernardinelli, G.; Wang, Y.; Spellmeyer, D. C.; Buda, A.; Houk, K. N. Torquoselectivity in the Electrocyclic Conversion of Benzocyclobutenes to o-Xylylenes. *J. Am. Chem. Soc.* **1992**, *114*, 1157−1165.

https://doi.org/10.1021/acs.inorgchem.2c00824
Inorg. Chem. 2022, 61, 14918−14923